A Unified Model of Optical and Physical Dot Gain in Print Color Reproduction

Li Yang▲

Campus Norrköping (ITN), University of Linköping, Norrköping, Sweden

A unified model coping with both physical and optical dot gains on print color tone reproduction is proposed. The physical dot gain, is approximated by a quadratic function of nominal dot percentages. The function, for each color, is characterized by a single parameter depending on printing technologies as well as ink–paper interactions, and has a symmetric form around where the nominal dot percentage is 50%. The parameter can be derived from the best fit for the model to measured data, such as spectral reflectance values or CIEXYZ tristimulus values. Applications to a color laser printer (on office copy paper) reproduces the experimental dot gain curves fairly well. Dependence on physical dot percentage, a summation of the nominal dot percentage and the corresponding physical dot gain, results in the optical dot gain and in turn the overall dot gain asymmetric forms, plotted against the nominal dot percentages. Furthermore, theoretical analysis reveals fundamental differences between physical and optical dot gains. Therefore, effects of optical dot gain can not be accurately represented by any physical extension in printing practices.

Journal of Imaging Science and Technology 48: 347–353 (2004)

Introduction

Color reproduction in printing is achieved by distributing (printing) colorants (inks, toners, etc.) onto a substrate surface. Ink setting on the surface is a complex process depending on the physical and chemical properties of the inks and the substrate, surface topology, etc. In electrophotographic systems like laser printers, toner deposition depends on toner transport and development (heating, fusing, and pressing) processes. In ink jet systems, this depends on interaction between the ink drops and the surface of the printed media. Considering the relief structure of the printed page, the interaction results in ink spreading as well as ink penetration.[1,2]

Physical dot gain refers to a fact that sizes of printed dots differ from their nominal ones (bigger or smaller) in printing practice. Physical dot gain can be caused by printing systems, such as pressing force for toner setting, or by environment, for instance in ink jet printing, ink setting depends on moisture and surface state of substrates.[3] In a well controlled environment, physical dot gain may be considered as a systematic characteristic resulting from a printing system including printers and print related materials. Therefore knowledge about physical dot gain of printing systems may be helpful for system calibration and quality control of color reproduction.

Besides the physical dot gain that results from a real physical extension of an ink dot, there exists dot gain of optical origin,[1,4] i.e., optical dot gain or the Yule–Nielsen effect. Optical dot gain results from light scattering inside the substrate, which leads to light exchange between different chromatic areas, Σ_0 and Σ_1, as shown in Fig. 1. Because the light exchange occurs most likely at regions close to the border between the different chromatic areas, optical dot gain is closely related to the physical shape of the dots. Such a correlation between optical and physical dot gain makes the study a complicated task. Although there have been different approaches describing optical dot gain,[5–13] experimental confirmation has been difficult because of difficulties in separating an optical dot gain from a physical one. Moreover quantitative evaluation of the pure effects from physical or from optical dot gain has been difficult.

Coexistence of optical and physical dot gains in a print requires development of a unified model that accounts for both types of dot gain simultaneously. In previous publications,[12,13] we developed a model that parameterized optical dot gain in mono- and multi-color printing processes with consideration of ink penetration. In this work we present a model that parameterizes physical dot gain. Based on these models a unified model characterizing both optical and physical dot gain is established. The model is further illustrated by applications to a laser printing system. Finally, correlations and fundamental differences between physical and optical dot gains are studied.

Original manuscript received September 19, 2003

▲ IS&T Member

phone: +46-1136-3069; fax: +46-1136-3270; email: liyan@itn.liu.se

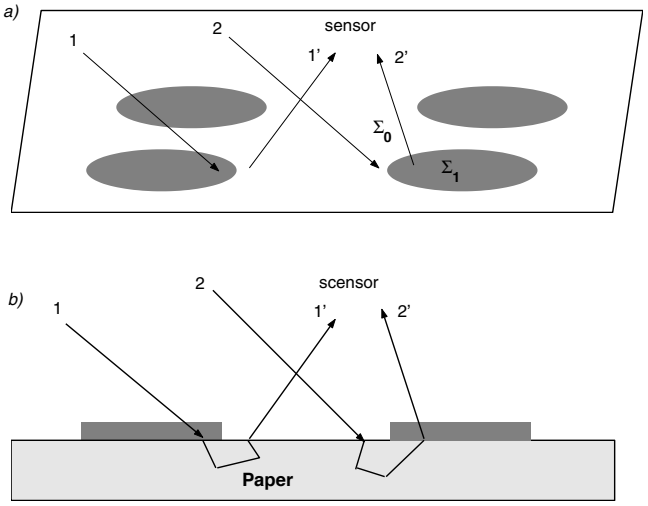

Figure 1. The Yule–Nielsen effect resulting from light scattering within the substrate. In the figure, light rays enter the substrate from one area (Σ_0 or Σ_1) and exit from another (Σ_1 or Σ_0).

Methods

Parameterization of Physical Dot Gain

Intuitively there exist correlations between the physical dot percentage, $\sigma = \sigma_0 + \Delta\sigma$, and the nominal one, σ_0. The correlation may mathematically be approximated by a polynomial expansion, for example a quadratic, i.e.,

$$\sigma = c + a\sigma_0 + b\sigma_0^2 \tag{1}$$

Considering constraints at $\sigma_0 = 0$ and 1, one gets,

$$c = 0$$
$$a + b = 1.$$

Then, Eq. (1) becomes,

$$\sigma = \sigma_0\,(a(1 - \sigma_0) + \sigma_0). \tag{2}$$

Consequently, the expression for physical dot gain is,

$$\Delta\sigma = \sigma - \sigma_0 = (a - 1)\,\sigma_0(1 - \sigma_0). \tag{3}$$

This means that the physical dot percentage, σ, or in turn the physical dot gain, $\Delta\sigma$, can be described by a single parameter, a, which depends on printing technology (offset or ink jet, etc.), printing materials (inks and substrates) used, and even printing environments, etc. Evidently, constraints for $\Delta\sigma = 0$ at $\sigma_0 = 0$ and 1, are automatically fulfilled in Eq. (3). The parameter, a, in Eq. (3) provides a measure of the physical dot gain. For example, $a = 1$ corresponds to no physical dot gain, while $a > 1$ or $a < 1$ stands for a physical dot extension ($\sigma > \sigma_0$) or a contraction ($\sigma < \sigma_0$), respectively.

Determination of Physical Dot Gain from Experimental Data

Let the nominal dot percentage be σ_0, which becomes $\sigma = \sigma_0 + \Delta\sigma$ after printing, due to physical dot gain. According to our previous work,[12,13] the spectral reflectance values of a print can be computed from

$$\begin{aligned} R(\sigma) &= R_{MD}(\sigma) - \Delta R_{opt}(\sigma) \\ &= R_{MD}(\sigma_0) - \Delta R_{phy}\,(\sigma_0) - \Delta R_{opt}(\sigma), \end{aligned} \tag{4}$$

where

$$R_{MD}\,(\sigma_0) = R_g\,(1 - \sigma_0) + R_g T^2 \sigma_0 \tag{5}$$

is the term computed with Murray–Davis equation. In Eq (5), R_g and T refer to spectral reflectance and transmittance values of paper and ink layers, respectively. ΔR_{phy} and ΔR_{opt} in Eq. (4) correspond to contributions of physical and optical dot gain, respectively and are expressed as

$$\begin{aligned} \Delta R_{phy}(\sigma_0) &= R_g(1 - T^2)\Delta\sigma \\ &= R_g(1 - T^2)\,(a - 1)\sigma_0(1 - \sigma_0) \end{aligned} \tag{6}$$

$$\Delta R_{opt}(\sigma) = \bar{p}(1 - T)^2\sigma(1 - \sigma) \tag{7}$$

where $\bar{p}$ is an average probability for light exchange between Σ_0 and Σ_1 (see Fig. 1), due to light scattering in the substrate, and is defined as

$$\bar{p} = \frac{1}{\sigma(1-\sigma)} \int_{\Sigma_1} \int_{\Sigma_0} p(\mathbf{r}_1, \mathbf{r}_0)\, d\sigma_1 d\sigma_0. \tag{8}$$

In the equation, $p(\mathbf{r}_1,\mathbf{r}_0)$ is the so-called point spread function (PSF) of the substrate, r_0 and r_1 denote positions where a photon enters and then exits the surface of the substrate. In case of complete light scattering, the photon has an identical probability to be scattered anywhere in the substrate. Then, $\bar{p}$ is constant and independent of the incident and exiting positions.[4,12] Consequently, the curve of optical dot gain has a single maximum at $\sigma = 50\%$ and has a symmetric form around the maximum. Nevertheless, when there also exists a physical dot gain, $\sigma \neq \sigma_0$, ΔR_{opt} becomes asymmetric around $\sigma_0 = 50\%$, when plotted against the nominal dot percentage, σ_0, as one will see below.

Correlation of the optical dot gain, ΔR_{opt}, with the physical dot gain is clearly seen from Eq. (7), because of its dependence on $\sigma = \sigma_0 + \Delta\sigma$. Since physical and optical dot gain contribute simultaneously to reflective measurements, an overall effect of dot gain, ΔR, is actually measured, which is a superposition of their contributions, i.e.,

$$\Delta R = \Delta R_{phy} + \Delta R_{opt} \tag{9}$$

According to Eqs. (4) through (9), in addition to the optical properties of paper and ink, R_g, $\bar{p}$, T, etc., the spectral reflectance, R (or the overall dot gain, ΔR) is determined by the parameter, a. Therefore, by fitting to a set of experimental data, such as reflectance values or CIEXYZ tristimulus values, one can determine the numerical value of a, and thus the physical dot gain, $\Delta\sigma$.

ΔR_{phy} and ΔR_{opt} are mathematically similar, but their differences are significant. ΔR_{phy} is parabolic with respect to the nominal dot percentage, σ_0, but ΔR_{opt} to the total dot percentage, σ, instead. In other words, $\Delta R_{opt,}$ responds to both the nominal σ_0 as well as the physical dot gain, $\Delta\sigma$. Consequently, ΔR_{phy} and ΔR_{opt} are symmetric about their maxima at $\sigma_0 = 50\%$ and $\sigma = 50\%$, respectively, in the case of $\bar{p} = constant$, i.e., light is isotopically scattered in the substrate. When ΔR_{opt} is plotted against the nominal dot percentage, σ_0, its maximum is shifted to a lower or higher σ_0 value, depending on whether $\Delta\sigma$

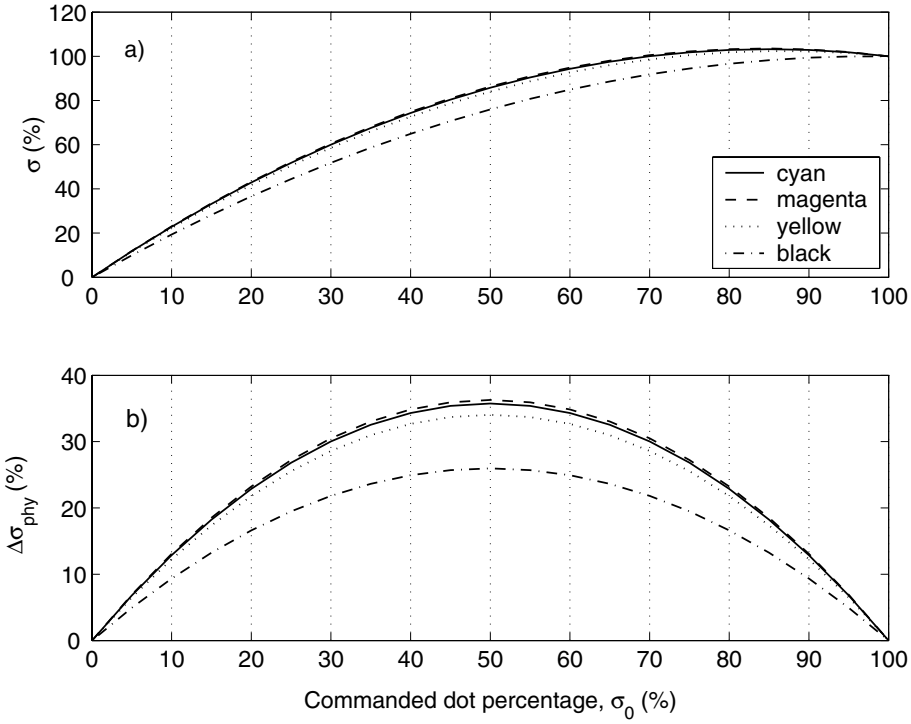

Figure 2. Variation of physical dot gain ($\Delta\sigma$) and printed dot percentage (σ) with respect to the nominal dot percentage (σ_0). Curves of cyan and magenta eventually overlap with each other.

is positive or negative. Correspondingly, the total dot gain, ΔR, is asymmetric because it is a simple summation of these two terms. Therefore, the asymmetry of the measured dot gain curve, ΔR, suggests the coexistence of physical and optical dot gain, as one can see in the next Section.

Results and Discussions

To illustrate applications of the model developed in the previous section, a laser printing system based on HP Color Laser Jet 4500N was studied. Test patches of primary colors and black were printed by the printer with nominal dot percentages ranging from 0 to 100% and an interval of 5%. Ordinary office copy paper was used for printing. Settings for the printer were 600 dpi with scale patterns.

Spectral reflectance values of the patches were obtained utilizing a spectrophotometer with a UV filter which covers spectral wavelengths ranging from 380 to 730 nm and an interval of 10 nm. Spectral transmittance values for each color, T, are estimated by

$$T = \left(\frac{R_1}{R_g}\right)^{1/2} \tag{10}$$

where R_1 is the spectral reflectance value of a full tone color. Applying Eq. (10), one must be aware of possible errors that may be associated with such a simple estimation. One of the possible errors comes from boundary reflections at air/ink and ink/paper interfaces which can be important for toner based colorants, because of different refractive indices of the ink and the air. One can cope with the boundary reflections by making the so-called Saunderson correction.[14] Another possible error relates to thickness variation of halftone dots. Determination of the thickness variation requires sophisticated microscopic studies,[3] which is beyond the scope of this work. Fluorescence of the substrate can also be a source of error when the UV filter is not sufficient, as may be the case in the present study. The simulation makes no attempt to exactly reproduce the measurement data rather to illustrate applications of the unified model. Nevertheless, since these possible errors are relatively less important compared to physical and optical dot gains, reasonable results from simulation can still be expected.

Simulations were evaluated by fitting the computed spectral reflectance values, R_{simu}, according to Eqs. (4–9), to the measurements, R_{exp}, using least squared error (LSQ), i.e.,

$$Q = \sum_{\lambda}\sum_{\sigma}\left[R_{simu}(\sigma,\lambda) - R_{\exp}(\sigma,\lambda)\right]^2, \tag{11}$$

as a figure of merit. Optical dot gain resulting from light scattering in the substrate was approximated by the complete light scattering, and $\bar{p} = R_g$ was assumed in the simulation. Therefore, for each color, there is only one parameter, a, describing physical dot gain of printed dots, involved in fitting processes.

The Dot Gain Curves

Figure 2 depicts variations of the physical dot gain, $\Delta\sigma$, and the physical (or real) dot percentage, σ, with respect to the nominal one, σ_0, for the primary colors as well as black. Figure 2(a) provides us with the correlation between the actual dot percentage and the nomi-

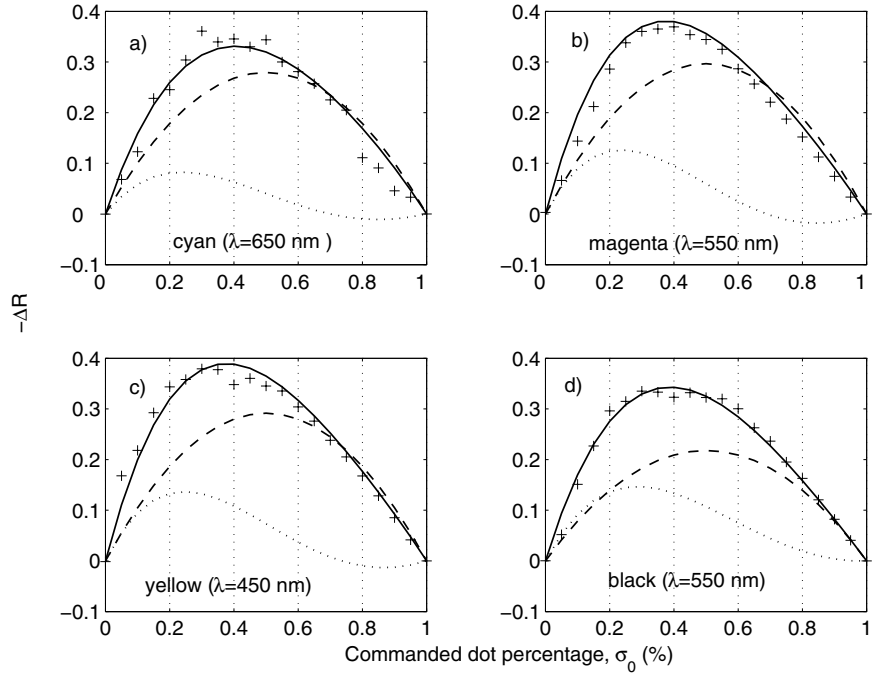

Figure 3. Effects of the physical (ΔR_{phy}), dashed line, optical (ΔR_{opt}), dotted line and overall (ΔR), solide line, dot gain on reflectance values. Experimental values of ΔR are marked by +.

nal values. As expected from the theoretical analysis, the physical dot gain (Fig. 2(b)) has a symmetric form about its maximum in mid tone, $\sigma_0 = 50\%$. The maximum physical gains range from $\Delta\sigma = 26\%$ to 36%, depending on colors. The dot gain is significant, particularly compared with its nominal value. Besides, cyan and magenta have eventually the same dot gain profile (they overlap with one another in the figure), while yellow and black have smaller and the smallest dot gain, respectively. The corresponding dot gain parameters are, $a = 2.4399$ (cyan), 2.4338 (magenta), 2.2907 (yellow), and 2.0335 (black).

Figure 3 further demonstrates contributions from the physical and optical dot gain, ΔR_{phy} and ΔR_{opt}, and their joint effects on overall spectral reflectance values, ΔR. Because of spectral dependence, ΔR values corresponding to different nominal dot percentages and at a wavelength lying in the middle of the main absorption band of each color were plotted. At these wavelengths (noted in the figure), both the physical and optical dot gains have their maxima, which provide one with possible ranges for how large the effects of dot gains may be.

Due to physical extension of the printed dot, $\Delta\sigma > 0$, in the experiments, the optical dot gain reaches its maximum at about $\sigma_0 = 25\%$ to 30%, for the primary colors and black. Also due to physical dot gain, the print (tone) becomes eventually solid when the nominal dot percentage is $\sigma_0 \simeq 80\%$ or higher, which leads to the vanishing of the optical dot gain. Additionally, ΔR_{opt} shares a similar shape for all colors since their transmittance values at the wavelengths lying in the middle of their absorption bands are similar ($T \approx 0$). Finally, superpositions of the physical and optical dot gains make the overall dot gain curves, ΔR, asymmetric with respect to their maxima which occur at about $\sigma_0 = 40\%$ for all colors. Experimental values of the overall dot gain are also included in Fig. 3, which agree fairly well with the simulations.

For a simpler comparison between the simulations and the measurements, both the simulated and experimental spectral reflectance values have been converted to their color coordinates in the CIEXYZ color space. These data are shown in Fig. 4, in which the simulations are represented by lines (solid, dashed, dotted, and dash–dot lines for cyan, magenta, yellow, and black, respectively) and the measurements by dots. The figure shows fairly good agreement between the simulations and the measurements, especially for X and Y. Figure 5 further provides a quantitative measure of the color differences between the simulated and experimental spectra. The plots show that for most colors and dot percentages, the color differences lie below $\Delta E = 6$ except for magenta whose maximum is $\Delta E = 11$. This implies that the quadratic approximation to the physical dot gain (Eq. 3) and the assumption of complete light scattering hold reasonably well for this printing system. As suggested in the previous section, the error may come from the following possible sources: the boundary reflection, the thickness variation of ink dots, and even fluorescence of the substrate, which were ignored in this model. Studies on other printing systems are necessary in order for a general conclusion can be drawn.

Spectral Dependence of the Optical Dot Gain

Because $\Delta R_{opt} > 0$, the true reflectance of an image, R, is smaller than its Murray–Davies value, R_{MD}, and the halftone image appears to be darker (more saturated in color). Equivalently, it appears as a larger dot percentage than physically obtains. For this reason this effect is known as optical dot gain.

In cases of complete light scattering, $\overline{p} = C$ (a constant where $C \leq 1$), which corresponds to the Yule–Nielsen model with a Yule–Nielsen factor, $n = 2$.[12] Correspondingly, the dot gain has its maximum at $\sigma = 50\%$, i.e.,

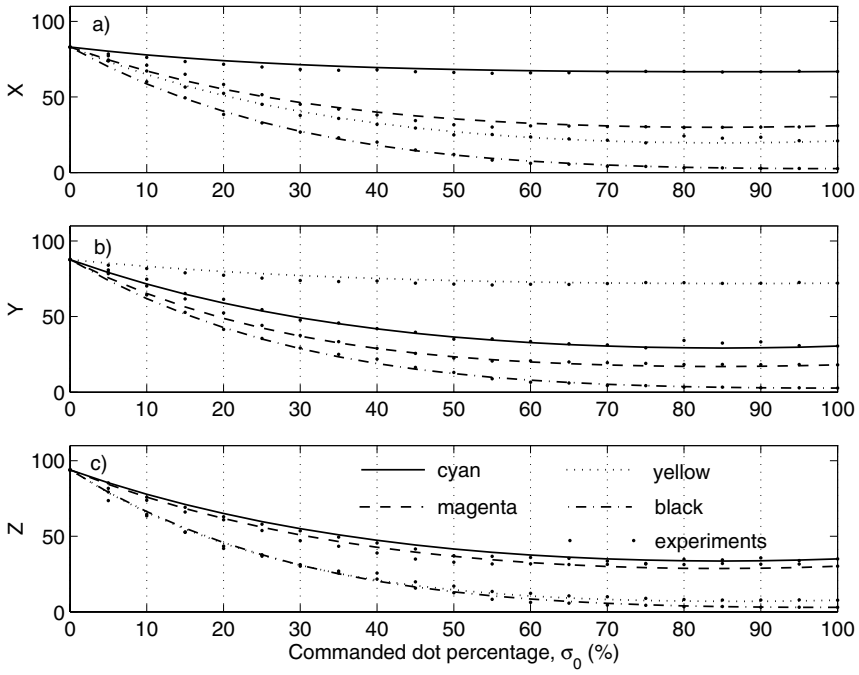

Figure 4. Simulated and measured (dots) CIEXYZ tristimuli values of cyan (solid lines), magenta (dashed lines), yellow (dotted lines), and black (dash–dot lines).

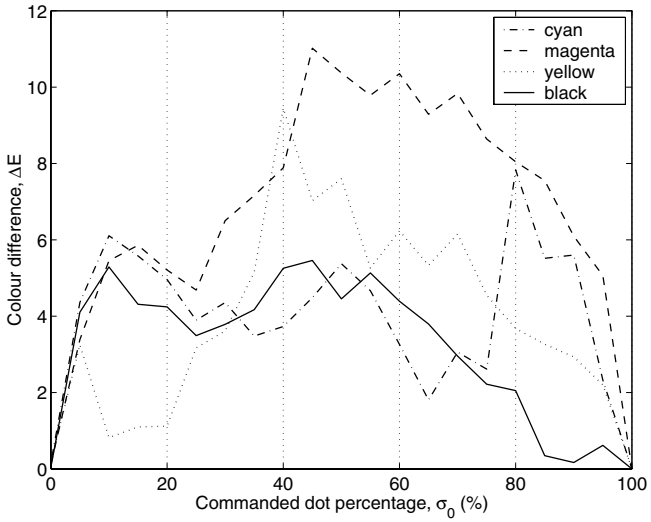

Figure 5. Color differences between simulated and measured spectra of cyan (solid lines), magenta (dashed lines), yellow (dotted lines), and black (dash–dot lines).

$$(\Delta R_{opt})_{\max} = (1 - T)^2 C/4 \tag{12}$$

In an extreme case, $T = 0$ and $C = 1$, one gets the largest possible optical gain, $(\Delta R_{opt})_{\max} = 0.25$.

The term 'optical dot gain' may give one an impression that it may be possible to represent an optical dot gain by a physical dot extension. If so, it would be possible to compensate the optical dot gain by making corrections in advance to an original. Consequently, perfect tone reproduction would be achievable. Unfortunately, the following analysis will show that such a compensation is not fully applicable over the whole spectrum, because of fundamental differences between optical dot gain and physical dot gain.

As an attempt to correlate effects of optical dot gain with a physical dot extension, $\Delta\sigma_{opt}$, one may consider the measured reflectance of dot percentage σ, $R(\sigma)$, as if it is originated from a dot size of $\sigma + \Delta\sigma_{opt}$. Therefore,

$$\begin{aligned} R(\sigma) &= R_{MD}(\sigma) - \Delta R_{opt}(\sigma) \\ &= R_{MD}(\sigma + \Delta\sigma_{opt}) \\ &= R_{MD}(\sigma) - R_g(1 - T^2)\Delta\sigma_{opt}. \end{aligned} \tag{13}$$

Applying expressions for R_{MD} and ΔR_{opt} (Eqs. (5) and (7)) one obtains,

$$\begin{aligned} \Delta\sigma_{opt} &= \frac{\Delta R_{opt}}{R_g\left(1 - T^2\right)} \\ &= \frac{(1-T)\bar{p}}{(1+T)R_g}\sigma(1-\sigma) \end{aligned} \tag{14}$$

Clearly, $\Delta\sigma_{opt}$ is a function of the optical properties (T, R_g) of the materials as well as ink percentage (σ). Due to spectral dependence, $\Delta\sigma_{opt}$ has its maxima in absorption bands where T is small but minima in transparent bands (where $T \to 1$). This makes optical dot gain differ fundamentally from physical dot gain. Therefore, except for an ideal black, where $T = 0$, an optical dot gain can not be properly represented by any single physical dot extension over the whole spectrum, even for primary colors.

To further demonstrate the spectral dependence, optical dot gains computed with to Eq. (12) is depicted in Fig. 6. In the calculation, $\sigma = 0.4$ and a complete light scattering was assumed. Clearly, $\Delta\sigma_{opt}$ shows a distinct correlation with its spectral transmittance, and the quantity $\Delta\sigma_{opt}$ varies significantly with the wavelengths.

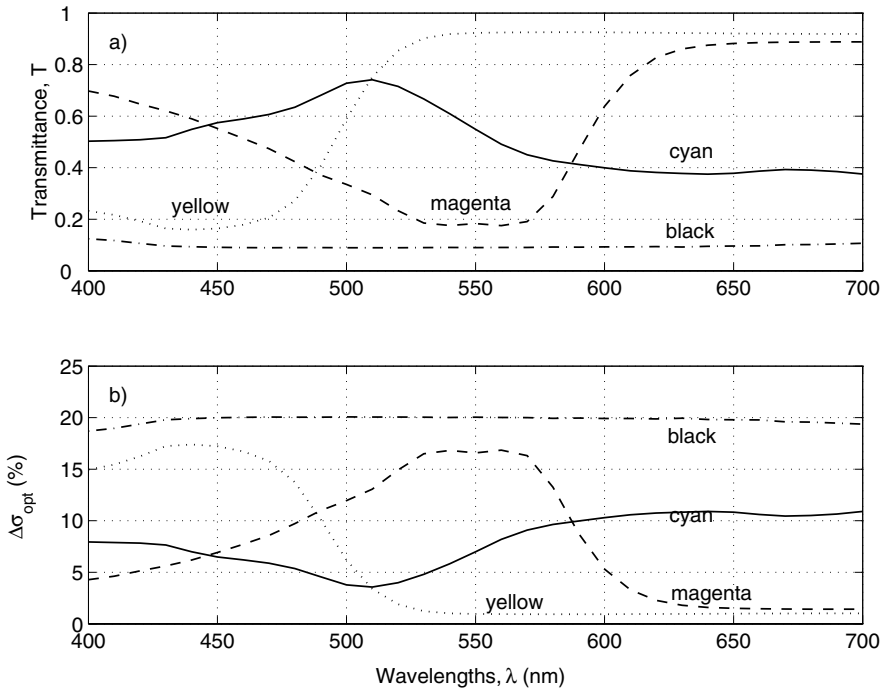

Figure 6. Spectral dependence of the pretended physical dot extension, $\Delta\sigma_{opt}$, resulting from effect of light scattering in the substrate. In the calculation, $\sigma = 0.4$ and the complete light scattering was assumed: a) spectral transmittance values of the toners; b) computed values of $\Delta\sigma_{opt}$ according to Eq. (12).

Remarks

Along with three other spectral models, the Clapper–Yule multiple internal reflection model, Beer–Bouger law, and Kubelka–Munk theory, the Yule–Nielsen model expressed as[15,16]

$$R(\lambda)^{1/n} = \sum_{i=1}^{N} w_i R(\lambda)^{1/n} \tag{15}$$

is possibly the most commonly used model.[17] The factor, n, is called the Yule–Nielsen factor and is obtained from best fit for the model to measurement data. The Yule–Nielsen (Y – N) equation is an empirical power-law correction to Murray–Davies model corresponding to $n = 1$. According to Ruchdeschel and Hauser,[18] $1 \le n \le 2$, when only optical dot gain is involved. This modification was originally aimed at accounting for effects of optical dot gain. Unfortunately, difficulties in separating physical from optical dot gain make the presumption of the Y–N equation seldom realized in applications. Consequently, the empirically derived Y–N factor can be significantly bigger than 2. For example, for a print created by an ink jet, possessing significant physical dot gain due to ink spreading, the best fit Yule–Nielsen factor[19] can be up to $n = 10$.

Numerous researchers have made great efforts to improve numerical accuracy of the Yule–Nielsen corrected Murray–Davies models, applied to predict spectral distributions and tristimulus values of color halftones.[20–26] However, these improvements depend on introducing more *Y–N* factors in regression processes, as for instance cellular Y–N models,[24–27] and therefore, do not provide more physical insight into real problems. Because of the coexistence of both physical and optical dot gains in measured data, the empirically derived Y–N factor, n, has no direct (or not much) physical meaning on its own. Moreover, as popularity of paper containing fluorescent whitening agents increases, physical interpretations of Y–N factors become even less clear.

The present model builds on solid physical ground, in which every parameter has a direct physical meaning on its own. It provides one with insight into the problems studied. For example, determination of physical dot gain can be used to calibrate printers in such a way as may be helpful for printer development and halftoning. Moreover, such a model building strategy provides ease of model extensions to include other physical effects like fluorescence of substrate, boundary reflection, etc. Detailed descriptions of an extension to prints on a substrate containing fluorescent agents will be reported elsewhere.[28] This will allow us to further test the model experimentally, by isolating one effect from others.

Summary

A model coping with both physical and optical dot gains in tone reproduction is derived. In the model, physical dot gain is approximated by a quadratic function of nominal dot percentage. For each color, the function is characterized by a single parameter depending on printing technology as well as ink–paper interactions. The parameter can be derived by fitting experimental data, say, spectral reflectance values of a set of test patches. The model reveals that physical dot gain, $\Delta\sigma$, has a parabolic form when plotted against nominal dot percentage (σ_0), and reaches its maximum around $\sigma_0 = 50\%$. The response (dependence) of the optical dot gain to the physical dot gain (dot extension) results in an asymmetric form of the optical dot gain, and, in turn, an asymmetric form of the overall dot gain. The model is applied to a color laser printer. The simulated dot gain curves

are in fairly good agreement with measurements. Theoretical analysis suggests that it is impossible to represent an optical dot gain by any single physical dot extension over the whole visible spectrum, because of spectral dependence of the optical dot gain.

Acknowledgment. This work is supported by Swedish Foundation for Strategic Research through Surface Science Printing Program (S2P2).

References

1. L. Yang, *Ink-Paper Interaction: A study in ink jet color reproduction*, Ph.D thesis, Dissertation No. 806, Linköping University, Sweden, 2003.
2. S. S. Hwang, Toner penetration into paper at fusing, *J. Imaging Sci. Technol.* **44,** 26 (2000).
3. P. Emmel and R. D. Hersch, Modeling ink spreading for color prediction, *J. Imaging Sci. Technol.* **46,** 237 (2002).
4. G. L. Rogers, Optical dot gain in a halftone print, *J. Imaging Sci. Technol.* **41,** 643 (1997).
5. J. S. Arney, A probability description of the Yule–Nielsen effect, I, *J. Imaging Sci. Technol.* **41,** 633 (1997).
6. J. S. Arney and M. Katsube, A probability description of the Yule–Nielsen effect II: The impact of halftone geometry, *J. Imaging Sci. Technol.* **41,** 637 (1997).
7. A. C. Hübler, The optical behavior of screened images on paper with horizontal light diffusion, in *Proc. IS&T's NIP-13: Int'l. Conference on Digital Printing Technologies*, IS&T, Springfield, VA, 1997, 506–509.
8. S. Gustavson, *Dot Gain in Color Halftones*, Ph. D. Thesis, Dissertation No. 492, Linköping University, Sweden, 1997.
9. G. L. Rogers, Effect of light scatter on halftone color, *J. Opt. Soc. Amer. A* **15,** 1813 (1998).
10. G. L. Rogers, Optical dot gain: lateral scattering probabilities, *J. Imaging Sci. Technol.* **42,** 341 (1998).
11. P. Emmel and R. D. Hersch, A unified model for color prediction of halftoned prints, *J. Imaging Sci. Technol.* **44,** 351 (2000).
12. L. Yang, R. Lenz and B. Kruse, Light scattering and ink penetration effects on tone reproduction, *J. Opt. Soc. Amer. A* **18,** 360 (2001).
13. L. Yang, S. Gooran and B. Kruse, Simulation of optical dot gain in multichromatic tone production, *J. Imaging Sci. Technol.* **45,** 198 (2001).
14. J. L. Saunderson, Calculation of the color of pigmented plastics, *J. Opt. Soc. Amer.* **32,** 727 (1942).
15. J. A. C. Yule and W. J. Nielsen, The penetration of light into paper and its effect on halftone reproduction, *TAGA Proc.* **3,** 65 (1951).
16. J. A. Viggiano, The color of halftone tints, in *TAGA Proc.*, 647–661 (1985).
17. A. U. Agar, Model Based Color Separation for CMYKcm Printing, *Proc. International Conf. Image Processing* (*ICIP 2000*), IEEE Computer Society, Los Alamitos, CA, 2000, and references therein.
18. F. R. Ruckdeschel and O.G. Hauser, Yule–Nielsen effect in printing: A physical analysis, *Appl. Opt.* **17,** 3376 (1978).
19. R. S. Berns, A. Rose and D. Y. Tzeng, *The spectral modeling of large-format ink jet printers,* Research and development final report, Munsell Color Science Laboratory, RIT, Rochester, New York, 1996.
20. K. J. Heuberger, Z. M. Jing and S. Persiev, Color transformations and lookup tables, *TAGA Proc.*, 863–881 (1992).
21. R. Rolleston and R. Balasubramanian, Accuracy of various types of Neugebauer model, *Proc. 1st IS&T/SID Color Imaging Conf.*, IS&T, Springfield, VA, 1993, pp. 32–37.
22. B. K. Lee, Estimation of the Neugebauer model of a halftone printer and its applications, in *Optics and Imaging in the Information Age Proceedings*, IS&T, Springfield, VA, 1996, pp. 376–379.
23. R. R. Balasubramanian, The use of spectral regression in modeling halftone color printers, in *Optics & Imaging in the Information Age*, IS&T, Springfield, VA, 1996, pp. 372–375.
24. S. L. Chang, Y. T. Liu and D. Z. Yeh, A model to estimate fractional areas of Neugebauer primary colors, *Proc. 5th IS&T/SID Color Imaging Conf.*, IS&T, Springfield, VA, 1997, pp. 97–100.
25. C. C. Hua and K. L. Huang, Advanced cellular YNSN printer model, *Proc. 5th IS&T/SID Color Imaging Conf.*, IS&T, Springfield, VA, 1997, pp. 231–234.
26. A. U. Agar and J. P. Allebach, A iterative cellular YNSN method for color printer characterization, *Proc. 5th IS&T/SID Color Imaging Conf.*, IS&T, Springfield, VA, 1997, pp. 197–200.
27. T. Ogasahara, Verification of the predicting model and characteristics of dye-based ink jet printer, *J. Imaging Sci. Technol.* **48**, 130–137 (2004).
28. L. Yang, Spectral model of halftone on a fluorescent substrate, to be submitted.